Short Papers

Green's Function Approach for Obtaining S-Matrices of Multimode Planar Networks

RAKESH CHADHA, MEMBER, IEEE, AND K. C. GUPTA, SENIOR MEMBER, IEEE

***Abstract*— Evaluation of S-matrices for circuits using multimode microstrip-like lines is presented. Planar waveguide model for lines and two-dimensional analysis using Green's functions are used. As an example, a multimode S-matrix is computed for a microstrip right-angled bend.**

I. Introduction

Two-dimensional microwave or millimeter-wave planar networks have planar transmission lines (such as striplines, microstrip lines, suspended microstrips, inverted microstrips, etc.) connected at various ports of the network. For the analysis of such circuits, planar-waveguide models may be employed for these transmission lines. Planar-waveguide models imply that the current density distribution for the lowest order mode is uniform over the effective width. At the discontinuity in the network, higher order modes are excited in the planar outgoing lines. At microwave frequencies, these higher order modes are usually evanescent and, hence, decay along the transmission line away from the network. For such cases, two methods have been reported for evaluation of S-matrices [1], [2]. In the method proposed by Miyoshi and Miyauchi [1], external ports are divided into subports, and voltage and current density along the width of a port are expanded into higher order modes. Since these higher order modes are evanescent, their characteristic impedances are reactive. The higher order modes are terminated in these reactive characteristic impedances at the port location itself. In an alternate procedure [2], sections of planar transmission lines are also considered as part of the network so that only the lowest order mode exists at the location of the port. In this method, the external ports need not be divided into subports.

At millimeter-wave frequencies, some of the higher order modes may not be evanescent and would propagate in the planar lines. This is especially true for wide lines or when the effective dielectric constant is high. In such cases, even though the signal at the input line is in the lowest order mode, the reflected wave and the waves coupled to other lines will, in general, have lowest order and higher modes. Different modes in a line are independent and can be treated as separate ports of the network. It is useful to know the coefficients relating wave variables for various modes at the external ports of the transmission lines. In this paper, a method useful for obtaining multimode scattering coefficients in such cases is described.

II. Method of Analysis

Consider a multiport planar network with planar transmission lines connected at the ports of the network. It is assumed that the reference planes for the external lines have been chosen far away from the geometrical discontinuities so that the evanescent modes are not present, that is, all the modes present are the propagating modes.

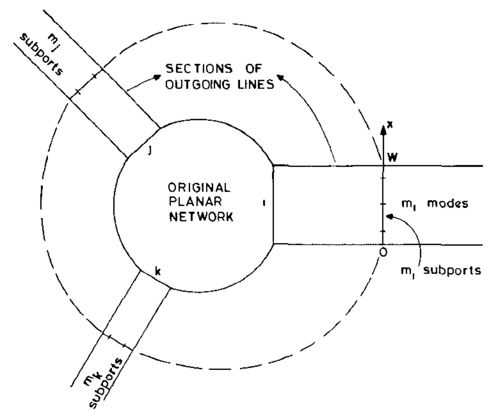

Fig. 1. Network configuration for multimode S-matrix evaluation

For multimode analysis, it is desirable to separate the voltages and currents of different modes propagating in the outgoing transmission lines. This separation can be carried out by dividing the external ports of the network into subports of smaller widths. The number of subports at each external port should be at least equal to the number of modes propagating in the transmission line so that the model parameters can be obtained by Fourier-series expansion. A similar procedure has been employed in [1] for considering evanescent higher order modes. The impedance matrix of the network (relating voltages and currents at the subports) may be evaluated using the Green's function approach and segmentation and desegmentation methods for simple shapes, and numerical methods for arbitrary shapes [3], [4]. In the Green's function approach, the planar shape is considered to be obtained from segments whose Green's functions are available. The resulting impedance matrix is obtained from those of the segments by using segmentation and/or desegmentation methods.

A. Modal Voltages and Currents

Let there be m propagating modes along any external line. The RF voltage $v(x)$ and current density $j(x)$ can be expanded in terms of m modes as [1]

$$v(x) = \sum_{k=1}^{m} p_k \cos\frac{(k-1)\pi x}{W} \tag{1}$$

$$j(x) = -\frac{1}{W}\sum_{k=1}^{m} q_k \cos\frac{(k-1)\pi x}{W} \tag{2}$$

where x is a running variable along the line width which extends from $x=0$ to $x=W$ as shown in Fig. 1. p_k and q_k are expansion coefficients for the kth mode. The Green's function approach used for obtaining the impedance matrix at various subports [3], [4] assumes that the current is distributed uniformly over the width of a subport and the voltage is the average voltage over its width. Thus, the assumed current density distribution in (2) needs

Manuscript received December 3, 1981; revised January 21, 1982.
R. Chadha is with the University of Waterloo, Waterloo, Ontario, Canada.
K. C. Gupta is with the University of Kansas, Lawrence, KS.

0018-9480/83/0200-0224$01.00 ©1983 IEEE

to be modified so that the current density is constant over the width of each subport. The modified current density distribution (denoted by $i_n(x)$) is obtained from (2) by taking its average over each subport. In the case of two subports of equal width with $m = 2$, the current density distribution gets modified as

$$i_n(x) = \begin{cases} -\frac{1}{W}\left(q_1 + \frac{2}{\pi}q_2\right), & \text{if } x < \frac{W}{2} \\ -\frac{1}{W}\left(q_1 - \frac{2}{\pi}q_2\right), & \text{if } x > \frac{W}{2}. \end{cases} \quad (3)$$

B. Normalization

The voltages and currents corresponding to different modes are obtained in terms of expansion coefficients p's and q's. For this purpose, all the modes are normalized. Total power flowing into a port is given by

$$P = -\int_0^W v(x)\, i_n(x)\, dx \quad (4)$$

where $v(x)$ is given by (1) and $i_n(x)$ is the modified current density. The power given by (4) must equal the total power in all the modes expressed as

$$P = v_1 i_1 + v_2 i_2 + \cdots + v_m i_m \quad (5)$$

where v_k and i_k refer to voltage and current corresponding to kth mode. Equating corresponding terms on the right-hand sides of (4) and (5), voltages v_k and currents i_k are expressed in terms of expansion coefficients p_k and q_k, respectively. The ratio v_k/i_k is kept equal to p_k/q_k.

It may be noted that this normalization is not needed for expansion in terms of higher order evanescent modes as used in [1].

C. Relationship Between Mode Parameters and Port Parameters

The voltages and currents at the subports are obtained using (1) and the modified current density distribution. At the jth subport

$$V_j = \frac{1}{W_j}\int_{W_j} v(x)\, dx \quad (6)$$

and

$$I_j = -\int_{W_j} i_n(x)\, dx. \quad (7)$$

It may be noted that $i_n(x)$ is constant over each subport. From (6) and (7), the voltages and currents at the subports can be expressed in terms of expansion coefficients p_k's and q_k's, respectively. On using normalization relations, which relate mode voltages and currents to p_k's and q_k's, we obtain matrices $\boldsymbol{C}$ and $\boldsymbol{D}$ so that

$$[V_1, V_2, \cdots, V_m]^t = \boldsymbol{C}[v_1, v_2, \cdots, v_m]^t \quad (8)$$

and

$$[I_1, I_2, \cdots, I_m]^t = \boldsymbol{D}[i_1, i_2, \cdots, i_m]^t \quad (9)$$

where V_j and I_j are subport parameters and v_k and i_k are mode parameters.

D. Evaluation of $\boldsymbol{C}$ *and* $\boldsymbol{D}$

Normally, a port is divided into subports of equal width. Evaluation of $\boldsymbol{C}$ and $\boldsymbol{D}$ is illustrated by considering a port of width W divided into m subports each of width W/m. Current density given by (2) is modified by taking its average over each subport and assuming it to be constant over the width of subport. The modified current density distribution $i_n(x)$, for x on the jth subport, is given by

$$i_n(x) = -\frac{1}{W}\sum_{k=1}^{m} q_k \cos\frac{(k-1)(2j-1)\pi}{2m}\, \text{sinc}\frac{(k-1)\pi}{2m},$$
$$\text{for } (j-1)\frac{W}{m} < x < j\frac{W}{m} \quad (10)$$

where $\text{sinc}\, x = (\sin x)/x$. Total power entering the port is expressed as

$$P = -\int_0^W v(x)\, i_n(x)\, dx$$
$$= \frac{1}{m}\sum_{k=1}^{m}\left[p_k q_k \text{sinc}^2\frac{(k-1)\pi}{2m} \cdot \sum_{j=1}^{m}\cos^2\frac{(k-1)(2j-1)\pi}{2m}\right]. \quad (11)$$

We have

$$\sum_{j=1}^{m}\cos^2\frac{(k-1)(2j-1)\pi}{2m} = \begin{cases} m, & \text{if } k=1 \\ m/2, & \text{if } 2 < k < m \end{cases} \quad (12)$$

and, hence, from (11) and (12)

$$P = p_1 q_1 + \frac{1}{2}\sum_{k=2}^{m} p_k q_k \text{sinc}^2\frac{(k-1)\pi}{2m}. \quad (13)$$

Comparing (5) and (13)

$$v_k = p_k \Delta_k \text{sinc}\frac{(k-1)\pi}{2m}$$
$$i_k = q_k \Delta_k \text{sinc}\frac{(k-1)\pi}{2m} \quad (14)$$

$$\Delta_k = \begin{cases} 1, & \text{if } k=1 \\ \frac{1}{\sqrt{2}}, & \text{if } 1 < k \leqslant m. \end{cases} \quad (15)$$

The voltage and current at a subport are obtained using (1), (6), (7), and (10) and are given as

$$V_j = \sum_{k=1}^{m} p_k \cos\frac{(k-1)(2j-1)\pi}{2m}\, \text{sinc}\frac{(k-1)\pi}{2m} \quad (16)$$

and

$$I_j = \frac{1}{m}\sum_{k=1}^{m} q_k \cos\frac{(k-1)(2j-1)}{2m}\, \text{sinc}\frac{(k-1)\pi}{2m} \quad (17)$$

where $(j-1)(W/m) < x < j(W/m)$. The elements of matrix $\boldsymbol{C}$ are obtained from (14) and (16) as

$$c_{jk} = \frac{1}{\Delta_k}\cos\frac{(k-1)(2j-1)\pi}{2m} \quad (18)$$

and

$$\boldsymbol{D} = \frac{1}{m}\boldsymbol{C}. \quad (19)$$

For $m = 2$ and $m = 3$, $\boldsymbol{C}$ may be written as

$$\boldsymbol{C}(m=2) = \begin{bmatrix} 1 & 1 \\ 1 & -1 \end{bmatrix} \quad (20)$$

and

$$C(m=3)=\begin{bmatrix} 1 & \sqrt{\frac{3}{2}} & \frac{1}{\sqrt{2}} \\ 1 & 0 & -\sqrt{2} \\ 1 & -\sqrt{\frac{3}{2}} & \frac{1}{\sqrt{2}} \end{bmatrix}. \tag{21}$$

Using (12), it can be found that

$$C^{-1}=\frac{1}{m}C^{t}. \tag{22}$$

E. Multimode S-Matrix

We can now treat different modes propagating in the planar lines also as separate ports. The matrices $\boldsymbol{C}$ and $\boldsymbol{D}$ are obtained for each planar transmission line. The multimode impedance matrix is given by

$$Z_m=\Gamma_1 Z_p \Gamma_2 \tag{23}$$

where Z_p is the impedance matrix at subports, Γ_1 and Γ_2 are block diagonal matrices whose submatrices on the diagonal are C_j^{-1} and D_j, respectively, and where j takes values from 1 to the number of outgoing transmission lines connected to the planar network. When all the subports at a port are of equal width, which is usually the case, both C_j^{-1} and D_j may be expressed in terms of $\boldsymbol{C}$ by using (19) and (22). The multimode scattering matrix can now be obtained from the multimode impedance matrix using characteristic impedances of various modes in different planar lines.

III. An Example

As an example, a multimode S-matrix is computed for a right-angled bend in microstrip. A right-angled bend occurs frequently in MIC's, and it is of interest to know the magnitude of higher order propagating modes above the cutoff frequency. Mehran [5] has studied bends of different angles and has reported dominant mode reflection and transmission coefficients until 40 GHz for a case when the first higher order mode cutoff frequency is 34 GHz.

For the computations reported here, Kompa's model for dispersion [6] in a microstrip is used[1]. At the bend, the line width is divided into six subports. Thus, six higher order modes are considered at the discontinuity. At the reference planes, the line width is divided into as many subports as the number of modes propagating in the line. The length of transmission line section on each side of the bend is considered such that the fields of the strongest evanescent mode at the reference plane have decayed to 1 percent of their magnitude at the bend. Using attenuation formula [7], this length is obtained as

$$l=\frac{0.733\lambda}{\sqrt{\left(\frac{n\lambda}{2W_e}\right)^2-1}} \tag{22}$$

where W_e is the effective width of the planar waveguide and n is the number corresponding to the evanescent mode with lowest cutoff frequency. For low frequencies when only the dominant mode propagates, $n=1$.

For a dominant mode excitation on one side of the bend, reflection and transmission in different modes are shown as functions of frequency in Fig. 2. Symbols ρ_d, ρ_h, and ρ_{h2} denote the reflection on the input line in dominant, first higher, and second higher modes, respectively. Similarly, τ_d, τ_{h1}, and τ_{h2} denote the transmission to the other line in dominant, first higher, and second higher modes, respectively. The dominant mode reflection and transmission coefficients agree with the results of Mehran [5], which are available only up to 40 GHz. Numerical results have also been computed for a bend in a planar waveguide with magnetic walls. For this case, the reflection and transmission in different modes is shown in Fig. 3. Symbols used are the same as those for the microstrip bend in Fig. 2.

[1]It is possible that the microstrip dispersion model used [6] is not very accurate at the discontinuity when higher order modes are propagating. However, the computations reported here are only as a representative example.

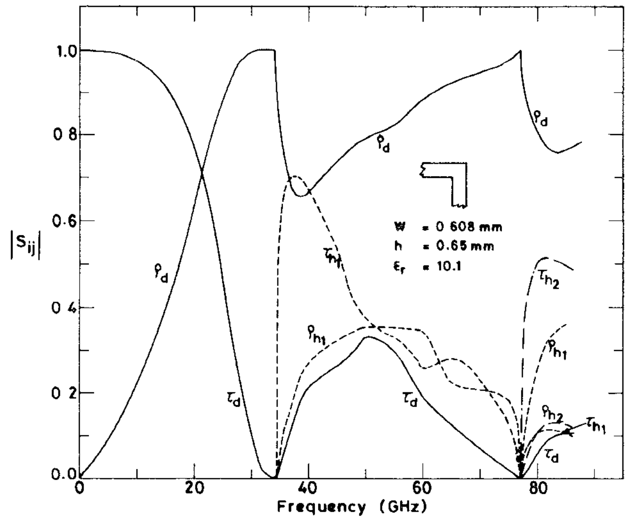

Fig. 2. Multimode transfer coefficients for a microstrip right-angled bend with input in lowest order mode.

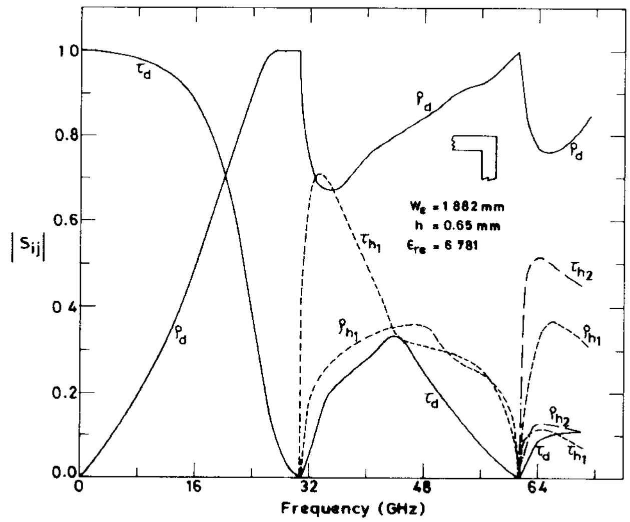

Fig. 3. Multimode transfer coefficients for a right-angled bend in a planar waveguide with magnetic walls and with input in lowest order mode.

IV. Discussion

A method for obtaining S-matrices for planar circuits where higher order modes could propagate has been presented. Planar waveguide models are needed for the transmission lines used. Using this method, the analysis of microstrip and stripline circuits can be extended to frequencies above the cutoff for higher order modes.

References

[1] T. Miyoshi and S. Miyauchi, "The design of planar circulators for wide-band operation," *IEEE Trans Microwave Theory Tech*, vol. MTT-28, pp. 210–214, Mar 1980.

[2] R. Chadha and K. C. Gupta, "Segmentation method using impedance matrices for the analysis of planar microwave circuits," *IEEE Trans. Microwave Theory Tech.*, vol. MTT-29, pp. 71–74, Jan. 1981.
[3] T. Okoshi and T. Miyoshi, "The planar circuit—An approach to microwave integrated circuitry," *IEEE Trans. Microwave Theory Tech.*, vol. MTT-20, pp. 245–252, Apr. 1972.
[4] K. C. Gupta, R. Garg, and R. Chadha, *Computer Aided Design of Microwave Circuits*. Dedham, MA: Artech House, 1981, chs. 8 and 11.
[5] R. Mehran, "Calculation of microstrip bends and Y-junctions with arbitrary angle," *IEEE Trans. Microwave Theory Tech.*, vol. MTT-26, pp. 400–405, June 1978.
[6] G. Kompa, "S-matrix computation of microstrip discontinuities with a planar waveguide model," *Arch. Elek. Ubertragung.*, vol. 30, pp. 58–64, 1976.
[7] S. Ramo, J. R. Whinnery, and T. Van Duzer, *Fields and Waves in Communication Electronics*. New York: Wiley, 1965, p. 421.

E-Plane *W*-Band Printed-Circuit Balanced Mixer

PAUL J. MEIER, SENIOR MEMBER, IEEE

***Abstract*—A balanced *W*-band mixer has been developed which integrates a low-loss printed-probe hybrid with fin-line diode mounts on a single substrate. This *E*-plane approach features production economy, effective shielding, high (> 400) unloaded *Q*, light dielectric loading, and simple waveguide interfaces. With the LO fixed at 95 GHz, the measured conversion loss of the mixer is 7.8±0.7 dB across the RF band of 92–98 GHz.**

I. Introduction

Continuing interest in the 3-mm atmospheric window has underscored the need for low-cost high-performance receivers. Balanced mixers are of special interest in radiometers where the IF is generally low, or in those applications where LO radiation must be minimized. A key component of a balanced mixer is the hybrid coupler which can be constructed in various forms. At millimeter wavelengths, the most common forms of printed-circuit hybrids have been the ring hybrid [1], the branch-line coupler [2], and the slot/coplanar/microstrip junction [3], [4]. Although existing designs can be scaled into the 3-mm band, problems are to be expected in terms of radiation, stray coupling, *Q* limitations, manufacturing tolerances, and interaction of waveguide transitions.

The printed-probe *E*-plane coupler has been developed [5], [6] as an alternative to the older forms of IC hybrids. A balanced mixer can be constructed entirely from *E*-plane lines [7] by integrating such a hybrid with fin-line diode mounts. Advantages of the *E*-plane approach at millimeter wavelengths include printed-circuit economy, negligible radiation and stray coupling, high unloaded *Q* (> 400 at 94 GHz), low-equivalent dielectric constant (for eased tolerances), and simple wide-band transitions to standard waveguide instrumentation.

This presentation reviews earlier component work [6], [7] that has not yet appeared in journal format, and describes the integration and performance of the balanced *E*-plane mixer.

II. Mixer Construction

Fig. 1 shows the *E*-plane *W*-band balanced mixer assembly. The major components, a seven-probe hybrid and a pair of fin-line diode mounts, are printed on a single board which is suspended in the *E*-plane of a four-port housing. All four ports were required in early tests of the hybrid alone. In the illustrated assembly only the two waveguide ports at the left are utilized. These ports serve as the RF and LO inputs. The IF outputs leave the housing through SMA connectors and are combined in a coax tee (not shown).

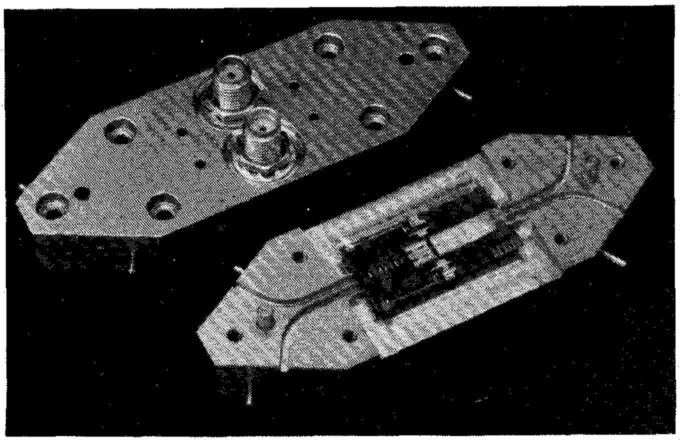

Fig. 1. *E*-plane balanced mixer.

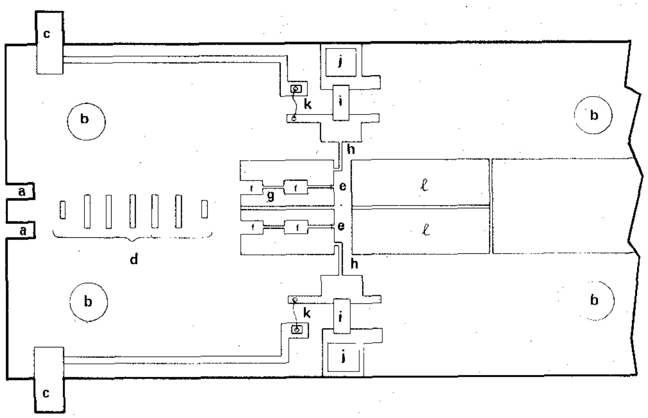

Fig. 2. Balanced mixer components.

Fig. 2 identifies the components of the printed-circuit assembly. Included are: a) quarter-wave notches which provide a match between the air-filled and slab-loaded waveguides, b) mounting holes which align the 5-mil, Duroid-5880 board within the housing, c) foil tabs where dc bias can be applied, d) seven-element printed-probe coupler, e) fin-line mounts for the beam-lead diodes, the mounts include f) RF transformers, g) gold wire that provides the ground return for the RF, LO, IF, and dc bias, h) IF output, containing high-impedance lines i) dc-blocking capacitors, j) connector contacts, k) resistors which block the IF from the dc bias circuit, and l) printed-circuit *E*-plane bifurcations which reactively terminate the diode mounts at RF and LO.

III. Printed-Probe Hybrid

At the center of the housing, shown in Fig. 1, parallel waveguides share a common broadwall. To accept a pair of dielectric boards, this broadwall is slotted. An array of coupling probes is printed on one board and insulated from the common wall by a second board that is fabricated from 2-mil Teflon.

The *E*-plane coupler was designed with the aid of the equivalent circuits shown in Fig. 3. The full circuit for a multielement coupler Fig. 3(a) can be reduced to the circuit of Fig. 3(b) for the modeling of isolated probes. The full circuit includes: a) genera-

Manuscript received March 16, 1982; revised May 26, 1982. This work was supported by Eaton Corporation's AIL Division.
The author is with the Eaton Corporation, AIL Division, Melville, NY 11747.